Infrared generation in low-dimensional semiconductor heterostructures via quantum coherence

A. A. Belyanin,[1,2] F. Capasso,[3] V. V. Kocharovsky,[1,2] Vl. V. Kocharovsky,[2]
and M. O. Scully[1,4]

[1]*Physics Department and Institute for Quantum Studies, Texas A&M University, College Station, Texas 77843*
[2]*Institute of Applied Physics, Russian Academy of Science, 46 Ulyanov Street, 603600 Nizhny Novgorod, Russia*
[3]*Bell Laboratories, Lucent Technologies, 600 Mountain Avenue, Murray Hill, New Jersey 07974*
[4]*Max-Planck Institute für Quantenoptik, 85748 Garching, Germany*

(Received 27 July 2000; published 11 April 2001)

A scheme for infrared generation without population inversion between subbands in quantum-well and quantum-dot lasers is presented. The scheme is based on the resonant nonlinear mixing of the optical laser fields on the two interband transitions that are generated in the same active region and that serve as the coherent drive for the infrared field. This mechanism for frequency down-conversion does not rely upon any *ad hoc* assumptions of long-lived coherences in the semiconductor active medium, and it should work efficiently at room temperature with injection current pumping. For optimized waveguide and cavity parameters, the intrinsic efficiency of the down-conversion process can reach the limiting quantum value corresponding to one infrared photon per one optical photon. Due to the parametric nature of infrared generation, the proposed inversionless scheme is especially promising for long-wavelength (far-infrared) operation.

DOI: 10.1103/PhysRevA.63.053803 PACS number(s): 42.55.Px

I. INTRODUCTION

Low-dimensional semiconductor heterostructures are almost ideally suited for generation in the mid- to far-infrared range (denoted below as IR for brevity), because the spacing between levels of dimensional quantization can be conveniently manipulated over the region from several to hundreds of microns, and injection pumping is possible. There is, however, a major problem: strong nonresonant losses of the IR field due to free-carrier absorption and diffraction, which become increasingly important at longer far-IR wavelengths. Due to the very short lifetime of excited states, it is difficult to maintain the large enough population inversion and high gain at the intersubband transitions necessary to overcome losses. There were many suggestions to solve this problem by rapid depletion of the lower lasing state using, e.g., the resonant tunneling to adjacent semiconductor layers or transition to yet lower subbands due to phonon emission [1,2], or even stimulated interband recombination [3]; see [4,5] for recent reviews. The successful culmination of these studies is the realization of quantum cascade lasers [2], in which the lower lasing state is depopulated either by tunneling in the superlattice or due to transition to lower-lying levels separated from the lasing state by nearly the energy of a LO phonon; see, e.g., [6] and references therein.

We here set forward another possibility, allowing us to achieve IR generation without population inversion at the intraband transition. This becomes possible with the aid of laser fields simultaneously generated at the *interband* transitions (called optical fields for brevity), which serve as the coherent drive for the frequency down-conversion to the IR. Employing self-generated optical lasing fields provides the possibility of injection current pumping and also removes the problems associated with external drive (beam overlap, drive absorption, spatial inhomogeneity), which were inherent in previous works on parametric down-conversion in semiconductors, see [4] for a review.

The second important feature is the great enhancement of nonlinear wave mixing near resonance with intersubband transitions. Note that the scheme of resonant terahertz generation by nonlinear mixing of two external laser fields in Sb-based quantum wells was recently studied by Liu *et al.* [7].

The third feature is the possibility of canceling the resonance one-photon absorption for the generated IR field due to coherence effects provided by self-generated driving optical fields [8]. The processes incorporating these three features constitute an important field of research with a variety of physical effects and promising applications. We consider just one example of such a process of IR generation and nonlinear mixing with self-generated optical fields in semiconductor heterostructures.

To avoid any misunderstanding, we note that the mechanism of IR generation discussed in this paper is different from the approach in which the resonant tunneling and Fano-type interference are used to establish a large coherence at intersubband transitions [9]. These quantum interference ideas usually imply the presence of a long-lived coherence at the intraband transitions. Our approach does not require long dephasing times. We here focus on a nonlinear wave-mixing phenomenon, which is greatly enhanced near the resonance with intersubband transition.

Note that this process has some common features with the recently observed generation of coherent IR emission in rubidium vapor in four-wave mixing experiments [10]. Also, coherent microwave generation at the difference frequency under the action of two resonant external optical fields was observed in cesium vapor [11]. In a recent paper [12] the use of the same scheme as in [11] was suggested for generation of terahertz radiation.

II. GENERIC THREE-LEVEL SCHEME

As the simplest case, consider the situation when only three levels of dimensional quantization are involved in gen-

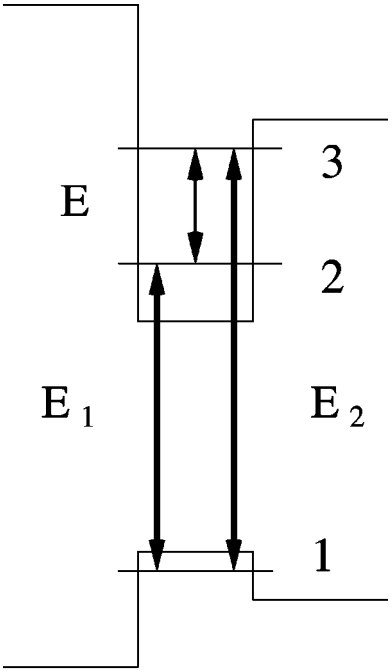

FIG. 1. Generic level scheme for three-color generation in an asymmetric quantum well: two strong fields E_1 and E_2 lasing at adjacent interband transitions $2\rightarrow1$ and $3\rightarrow1$ generate coherent IR radiation E at the beat frequency.

eration: one (lowest-lying) heavy-hole level, and two electron levels; see Fig. 1. Of course, this scheme also describes the situation when there are two hole levels and one electron level involved.

We will employ a simplified free-carrier model of a semiconductor active medium in which collision integrals describing electron-electron and electron-phonon scattering are replaced by terms with phenomenological relaxation and pumping rates. However, we do take full account of a semiconductor band structure when calculating the electron wave functions, energy levels, and dipole moments of interband and intersubband transitions. For this purpose, we employ the well-known Kane model [13], which takes into account the interaction of a conduction band with heavy-hole (hh), light-hole (lh), and split-off bands. The calculated values of dipole moments are used for numerical estimates of the IR intensity. Model equations and a more detailed discussion of the main approximations are presented in Sec. III.

We need all three transitions to be allowed by selection rules. In a quantum well (QW) this will generally require using asymmetric structures, e.g., a rectangular well with different barrier heights. For example, in an $Al_{0.3}Ga_{0.7}As/GaAs/Al_{0.2}Ga_{0.8}As$ QW of width 8-nm parametric IR generation is possible either between two electron subbands $1e$ and $2e$ separated by 100 meV ($\lambda\simeq12$ μm) or between the two lowest heavy-hole subbands ($\lambda\simeq70$ μm). Our calculations based on the Kane model show that it is advantageous to use asymmetric double QWs with intermediate semitransparent barriers. The ratio of dipole moments of $e1$-hh1 and $e2$-hh1 transitions can be about 3 for a wide range of parameters.

Symmetric QWs can also be employed, e.g., under a strong dc field bias or in the case of a strong coupling between different subbands of heavy and light holes. A typical example is the $Al_{0.3}Ga_{0.7}As/GaAs/Al_{0.3}Ga_{0.7}As$ QW in which the second subband of heavy holes 2hh and the first subband of light holes 1lh happen to be very close to each other (within homogeneous linewidth) in the Γ point for a wide range of thicknesses $\sim5-8$ nm, and therefore are strongly mixed. In this case two optical fields correspond to $1e\rightarrow1$hh and $1e\rightarrow1$lh transitions, and the IR field is generated via the $1\text{hh}\rightarrow2\text{hh}$ transition.

The third configuration of interest is a quantum dot (QD). For example, in a self-assembled InAs/GaAs quantum dot (QD) the three-level scheme can be easily realized with all three transitions allowed [14].

When the injection current density reaches the threshold value j_{th}, optical generation starts due to recombination transitions between ground electron and hole states. Upon increasing the pumping current, optical generation can start also from excited states and the laser can be completely switched to lasing from the excited state which has a higher maximum gain due to a larger density of states. The effect of excited-state lasing was studied both in QW and QD lasers [4,14–16]. It was found that with optimized laser parameters the region of simultaneous ground-state and excited-state lasing can be around $j\sim2j_{\text{th}}$ [15,16]. In order to have the region of two-wavelength lasing sufficiently broad [$\Delta j\sim(0.1-0.2)j_{\text{th}}$], gains for the two wavelengths should be close to each other.

The presence of one or two strong optical driving fields in the cavity gives rise to a rich variety of *resonant* coupling mechanisms by which the IR field can be produced. Here we will concentrate on one such scheme in which the two coherent optical fields having frequencies ω_1 and ω_2 excite the induced electronic oscillations at the difference frequency $\omega_2-\omega_1$. It is important to note that the coherent IR polarization is parametrically excited independently on the sign of the population difference at the IR transition.

The resulting output intensity of IR radiation depends on the coupling coefficient between the IR polarization and the cavity modes. It is clear that the polarization wave has a longitudinal wave number k_x equal to the difference $k_{2x}-k_{1x}$ of longitudinal wave numbers of the two optical fields. Therefore, only the mode having the above wave number is efficiently excited (the phase-matching condition). The field intensity is maximized when the frequency of this mode is equal to the difference frequency of optical fields. This requires special waveguide design since the refractive indices of bulk semiconductor materials for optical and IR frequencies are different. For far-IR generation, there is more flexibility due to the efficient manipulation of the refractive index by a slight doping.

III. BASIC MODEL

To quantify the above ideas, we have calculated the excited IR polarization and field by solving the coupled elec-

tronic density-matrix equations and electromagnetic Maxwell equations for the three fields, assuming steady state. It is convenient to expand all fields in an orthonormal set of cavity modes $\mathbf{F}_\lambda$ and to introduce slowly varying complex amplitudes of fields and polarizations. For example, for the IR field at the $3\rightarrow 2$ transition we can write

$$\mathbf{E}(\mathbf{r},t)=\sum_\lambda \frac{1}{2}\mathcal{E}_\lambda(t)\mathbf{F}^\lambda(\mathbf{r})\exp(-i\omega t)+\text{c.c.} \tag{1}$$

We will assume that the mode has a simple $\exp(\pm ik_x x)$ dependence in the propagation direction x with the refractive index $\mu=k_x c/\omega$ and the transverse structure defined by a specific waveguide.

After introducing the complex Rabi frequency $e(t)=d\mathcal{E}(t)/2\hbar$, the field equation for a given mode can be written as

$$\frac{de}{dt}+[\kappa+i(\omega_c-\omega)]e=\frac{2\pi i\omega d^2 N}{\hbar\mu^2}\int_{V_c}\sum_j \sigma_{32}^j F(\mathbf{r})d^3r. \tag{2}$$

Here d is the dipole moment of the IR transition, N is the total volume density of electron states in the active region, ω_{32} is the central frequency of $3\rightarrow 2$ transition, ω_c is the frequency of the IR cavity mode with given k_x, κ is the cavity loss, and V_c is the cavity volume. The variable σ_{32}^j is the slowly varying amplitude of the element ρ_{32}^j of density matrix, and the index j labels different electron states contributing to the inhomogeneously broadened line. For a system of QDs, j is simply the dot label. In QWs, index j labels different $\mathbf{k}_\parallel$ states with respect to longitudinal quasimomentum. Only $\mathbf{k}_\parallel$-conserving transitions are considered, where $\mathbf{k}_\parallel$ lies in the plane of the wells (xy plane).

The same representation is assumed for the two optical fields $\mathbf{E}_{1,2}$, with the corresponding parameters μ, d, ω, ω_c, κ, k_x, g having the index 1 or 2,

$$\frac{de_1}{dt}+[\kappa_1+i(\omega_{c1}-\omega_1)]e_1 = \frac{2\pi i\omega_1 d_1^2 N}{\hbar\mu_1^2}\int_{V_c}\sum_j \sigma_{21}^j F_1(\mathbf{r})d^3r, \tag{3}$$

$$\frac{de_2}{dt}+[\kappa_2+i(\omega_{c2}-\omega_2)]e_2 = \frac{2\pi i\omega_2 d_2^2 N}{\hbar\mu_2^2}\int_{V_c}\sum_j \sigma_{31}^j F_2(\mathbf{r})d^3r. \tag{4}$$

Note that the optical fields can have *arbitrary* polarization with respect to the parametrically excited IR field. In particular, for a QW laser the IR field is typically z polarized, while the optical fields are preferentially y polarized.

Expressions for σ_{ik} and population differences $n_{ik}=\rho_{ii}-\rho_{kk}$, $i,k=1,2,3$, are found from the density-matrix equations with phenomenological rates of relaxation and pumping,

$$\begin{aligned}
d\sigma_{21}/dt+\Gamma_{21}\sigma_{21}&=ie_1 n_{12}-ie_2\sigma_{32}^*+ie^*\sigma_{31},\\
d\sigma_{31}/dt+\Gamma_{31}\sigma_{31}&=ie_2 n_{13}-ie_1\sigma_{32}+ie\sigma_{21},\\
d\sigma_{32}/dt+\Gamma_{32}\sigma_{32}&=ien_{23}-ie_1^*\sigma_{31}+ie_2\sigma_{21}^*,
\end{aligned} \tag{5}$$

where

$$\begin{aligned}
\Gamma_{21}&=\gamma_{21}+i(\omega_{21}+\delta_j-\omega_1),\\
\Gamma_{31}&=\gamma_{31}+i(\omega_{31}+\delta_j-\omega_2),\\
\Gamma_{32}&=\gamma_{32}+i(\omega_{32}+\delta_j-\omega_2+\omega_1).
\end{aligned} \tag{6}$$

Here all sigmas and gammas should have the index j which was omitted to shorten notations. The quantity δ_j is the difference between the transition frequency for a given jth state and the central frequency ω_{21}, ω_{31}, or ω_{32}. The population differences $n_{ik}=\rho_{ii}-\rho_{kk}$ are defined from Eqs. (2)–(6) together with the three equations for ρ_{ii}, $i=1,2,3$, with phenomenological rates of population relaxation and pumping, shown below.

We note that this is a greatly simplified description of the complex many-body dynamics of carriers in the $\mathbf{k}$ space since all scattering processes are incorporated in the $\mathbf{k}$-independent phenomenological relaxation rates. Basically, the semiconductor active medium is treated here as an effective three-level medium with inhomogeneous broadening due to the distribution of carriers in the $\mathbf{k}$ space and possible structure imperfectness. At the same time, energy levels, wave functions, and dipole moments of the optical transitions are calculated by fully taking into account the semiconductor band structure. Namely, we use a Kane model [13] of four interacting bands in the Γ point. Such a simplified picture usually grasps well enough the main features of the resonant interaction between electromagnetic fields and electron-hole oscillators, and reproduces reasonably well the basic parameters of steady-state laser generation, such as the threshold pumping or output intensity of laser radiation; see, e.g., [17] for the detailed discussions. That is why the models of this type are so widely employed in calculations of semiconductor laser dynamics. Of course, spectral peculiarities of the observed emission resulting from collective excitations, band-gap renormalization, and other many-body effects cannot be described within this model. Realistic treatment of the carrier transport is also needed in order to describe transient processes on time scales comparable to the carrier thermalization time scale which is of the order of 100 fs.

For QW lasers the rates of spontaneous interband and intersubband transitions and injection pumping are usually much slower than the rate of intrasubband scattering which tends to bring the subband populations to quasithermal equilibria. Therefore, we can represent the phenomenological rate equations for populations in the following way [17]:

$$d\rho_{11}/dt + r_1(\rho_{11} - \overline{\rho}_{11}) = -2\,\mathrm{Im}[e_1^*\sigma_{21}] - 2\,\mathrm{Im}[e_2^*\sigma_{31}],$$

$$d\rho_{22}/dt + r_2(\rho_{22} - \overline{\rho}_{22}) = 2\,\mathrm{Im}[e_1^*\sigma_{21}], \tag{7}$$

$$d\rho_{33}/dt + r_3(\rho_{33} - \overline{\rho}_{33}) = 2\,\mathrm{Im}[e_2^*\sigma_{31}].$$

Here r_i, $i=1,2,3$ are the rates of intrasubband scattering and $\overline{\rho}_{ii}(\delta_j)$ are the distributions of populations supported by pumping in the absence of strong laser fields. They are expected to be close to Fermi-Dirac distributions with quasi-Fermi levels defined by the balance of pumping and spontaneous transitions. Very intense laser fields burn narrow spectral holes in the smooth and broad electron distributions. These holes, however, tend to be quickly refilled by scattering from neighboring parts of particle distribution. Note that this ''pumping'' to the spectral bandwidth involved in generation can proceed much faster than the external injection pumping which supports the total electron population.

For self-assembled quantum dot lasers, there is still a controversy regarding the efficiency of interaction between carriers bound in the dots and free electrons in the two-dimensional wetting layer. In the simplest case, we can consider the quantum dot as an atomlike system and we write for the jth dot

$$d\rho_{11}/dt = -2\,\mathrm{Im}[e_1^*\sigma_{21}] - 2\mathrm{Im}[e_2^*\sigma_{31}] + r_{21}\rho_{22} + r_{31}\rho_{33} - R_1\rho_{11},$$

$$d\rho_{22}/dt = 2\,\mathrm{Im}[e_1^*\sigma_{21}] + r_{32}\rho_{33} - r_{21}\rho_{22}, \tag{8}$$

$$d\rho_{33}/dt = 2\,\mathrm{Im}[e_2^*\sigma_{31}] + R - (r_{31} + r_{32})\rho_{33},$$

where r_{ik} are the relaxation rates of transitions $i \to k$, R is the rate of pumping to level 3, and R_1 is the rate of removal of electrons from level 1. For simplicity, we will assume bipolar injection with equal injection rates of electrons to level 3 and holes to level 1, so the total particle density is conserved. Note that this requires $R = R_1\rho_{11}$.

The solution of Eqs. (2)–(7) or Eqs. (2)–(6) and (8) in the steady state is straightforward but rather cumbersome. If the Rabi frequency of the IR field is much smaller than all γ_{ik}, we can retain only the terms in the zeroth and first order with respect to e and obtain for the induced polarization at IR transition

$$\sigma_{32}(\nu_j) \simeq \frac{e_2 e_1^*}{\tilde{\Gamma}_{32}}\left(\frac{n_{12}}{\Gamma_{21}^*} + \frac{n_{13}}{\Gamma_{31}}\right) + eF(\nu_j), \tag{9}$$

where

$$\tilde{\Gamma}_{32} = \Gamma_{32} + \frac{|e_1|^2}{\Gamma_{31}} + \frac{|e_2|^2}{\Gamma_{21}^*}, \tag{10}$$

$$F(\nu_j) = \frac{in_{23}}{\tilde{\Gamma}_{32}} + \frac{i|e_1|^2 n_{12}}{\Gamma_{21}\Gamma_{31}\tilde{\Gamma}_{32}} - \frac{i|e_2|^2 n_{13}}{\Gamma_{21}^*\Gamma_{31}^*\tilde{\Gamma}_{32}} + \frac{i|e_1|^2|e_2|^2}{|\tilde{\Gamma}_{32}|^2}\left(\frac{1}{\Gamma_{21}^*\Gamma_{31}^*} - \frac{1}{\Gamma_{21}\Gamma_{31}}\right)\left(\frac{n_{13}}{\Gamma_{31}^*} + \frac{n_{12}}{\Gamma_{21}}\right). \tag{11}$$

The expression (9) for the IR polarization contains two contributions of different origin. The first two terms are not proportional to e and describe the induced oscillations due to the mixing of two strong optical fields. The remaining terms that are proportional to the IR field e look rather lengthy. However, the physical meaning of each term in Eq. (11) is transparent. The first term is just the resonant one-photon absorption proportional to the population difference n_{23} at the IR transition. The second term in Eq. (11), which originates from the product $e_1^*\sigma_{31}$ in Eq. (5), is due to the mixing of the optical field e_1 and polarization σ_{31}, where the latter is excited by a two-photon term $\sigma_{31} \propto e\sigma_{21} \propto ee_1 n_{12}$. This way of exciting the σ_{32} coherence corresponds to the well-known ''ladder scheme'' of inversionless lasing [8,18]. The third term in Eq. (11) comes from the product $e_2\sigma_{21}^*$ and is also due to the mixing of two optical-frequency oscillations. Here the polarization σ_{21}^* is excited by a Raman-type two-photon term proportional to $e\sigma_{31}^*$, where, in turn, $\sigma_{31}^* \propto e_2^* n_{13}$. The resulting contribution to the IR polarization is proportional to $|e_2|^2 n_{13}$ and corresponds to the ''Λ scheme'' [8]. The remaining terms in Eq. (11) correspond to multiphoton processes of higher order and require the presence of two strong optical fields. For example, the term proportional to $|e_1|^2|e_2|^2 n_{13}$ comes partially from the product $e_1^*\sigma_{31}$, where $\sigma_{31} \propto ee_2\sigma_{32}^*$ and $\sigma_{32}^* \propto e_1 e_2^* n_{13}$ is, in turn, induced by the mixing of two strong optical fields. The origin of other terms can be easily followed in the same way.

The amplitude of the IR field can be written as

$$e \simeq \frac{ig^2 e_1^* e_2}{\kappa + \tilde{\kappa}} \sum_j \left(\frac{n_{12}(\nu_j)}{\Gamma_{21}^*\tilde{\Gamma}_{32}} + \frac{n_{13}(\nu_j)}{\Gamma_{31}\tilde{\Gamma}_{32}}\right), \tag{12}$$

where

$$g^2 = \frac{2\pi\omega d^2 NG}{\hbar\mu^2}$$

is the coupling coefficient between the IR field and polarization, and the term

$$\tilde{\kappa} = -ig^2 \sum_j F(\nu_j) \tag{13}$$

describes the linear susceptibility with respect to the IR field. Here G is the optical confinement factor for the IR field which measures the overlap of the mode field distribution with an active region.

In Eq. (12) an exact resonance $\omega_c=\omega_3-\omega_2$ with a given cavity mode having the wave number $k_x\simeq k_{2x}-k_{1x}$ is assumed. Otherwise, κ should be replaced by $i(\omega_c-\omega)+\kappa$.

The population differences n_{12}, n_{13} can be found from Eqs. (7) or (8) after substituting the expressions for σ_{21} and σ_{31}. The general form of the resulting expressions for n_{12}, n_{13} as functions of δ_j and $e_{1,2}$ is the same both in the model described by Eqs. (7) and in the model (8). This is because the terms describing stimulated transitions are the same in both cases. Therefore, we will use for definiteness the ''QW-like'' model described by Eqs. (7).

According to the discussion after Eq. (11), the quantity $\mathrm{Re}\,\tilde{\kappa}$ with $F(\nu)$ taken from Eq. (11) represents resonant IR-absorption losses modified by the presence of two strong optical fields. Its value can be negative in the absence of population inversion. This implies the possibility of ''true'' lasing without inversion: exponential amplification of a weak IR field from spontaneous noise. Unlike the nonlinear parametric process, this can happen even when only *one* of these two fields is present. In this case we have an already becoming ''classical'' ladder-type (Λ-type) scheme of inversionless lasing [8,18], in which, however, the driving field is not imposed externally, but is self-generated in an active medium. Inversionless lasing in semiconductors with a self-generated drive field is studied elsewhere [19]. Here we will ignore this possibility and neglect the corresponding term $|\tilde{\kappa}|$ in Eq. (12) as compared with the nonresonant losses κ at the IR wavelength.

In the general case, the problem should be solved numerically. However, significant simplification is possible for realistic laser parameters in some limiting cases, which will allow us to obtain the expression for the IR intensity showing its dependence on the main parameters; see Sec. IV.

IV. EFFICIENCY OF IR GENERATION

In this section we present estimates for the generated IR field intensity under the action of two strong laser fields. But first of all, let us indicate typical values of parameters entering the above equations. For definiteness, we will have in mind $Al_xGa_{1-x}As/GaAs$ QWs and InAs self-assembled QDs grown on GaAs or $Al_xGa_{1-x}As$ layers.

The value of the dipole moment at the IR transition is typically $d\sim(1-3)$ nm, while it is (0.3-1) nm for the optical transitions [4,14]. The relaxation rates γ_{ik} of both optical and IR polarizations are of order 5–10 meV in QW lasers at room temperature (i.e., the relaxation time $\lesssim 0.1$ ps) [17,20,21] and can be several times lower in self-assembled QDs (1 ps). In the IR range the cavity losses are mainly due to free-carrier absorption. At the high-carrier densities $N\gtrsim 10^{18}$ cm^{-3} necessary for the excited-state lasing in QWs the material losses in a bulk active medium are of order 100 cm^{-1} at $\lambda\simeq 6$ μm, and grow as λ^2 or λ^3 depending on the dominant scattering mechanism [22]. Thick cladding layers have a smaller doping density of order 4×10^{16} to 4×10^{17} cm^{-3}, but can contribute significantly to the losses due to the large overlap factor $G\sim 1$. Large losses are a major problem in all proposed far-IR lasing schemes involving free carriers in semiconductors. Note, however, that increasing losses are not a principal limitation in the present parametric scheme since they do not prohibit generation itself, but rather they decrease the IR field intensity. This possibility of far-infrared operation is an important advantage of the proposed mechanism. Note also that in QD lasers the excited-state lasing can be achieved at lower carrier densities due to the state filling effect, and the intrinsic losses in the active medium are lower.

A. Homogeneous broadening

This case can be relevant for the high-quality QWs and QDs. The main reasons for inhomogeneous broadening in QWs are growth defects leading to interface roughness, fluctuations in the well widths, and barrier heights. As for the self-assembled QDs, present-day structures have a large inhomogeneous broadening $\gtrsim 20$ meV associated with the spread of dot sizes, which is definitely much larger than the homogeneous linewidth.

For purely homogeneous broadening in the steady steate, and exactly at resonance $\omega_1=\omega_{21}$ and $\omega_2=\omega_{31}$, density-matrix equations together with wave equations for the fields $e_{1,2}$ yield

$$\frac{\kappa_1}{g_1^2}=-\frac{n_{12}}{\gamma_{21}}+\frac{|e_2|^2}{\gamma_{21}\tilde{\gamma}_{32}}\left(\frac{n_{13}}{\gamma_{31}}+\frac{n_{12}}{\gamma_{21}}\right),$$

$$\frac{\kappa_2}{g_2^2}=-\frac{n_{13}}{\gamma_{31}}+\frac{|e_1|^2}{\gamma_{31}\tilde{\gamma}_{32}}\left(\frac{n_{13}}{\gamma_{31}}+\frac{n_{12}}{\gamma_{21}}\right), \tag{14}$$

where

$$\tilde{\gamma}_{32}=\gamma_{32}+|e_1|^2/\gamma_{31}+|e_2|^2/\gamma_{21},$$

$$g_1^2=\frac{2\pi\omega_1 d_1^2 NG_1}{\hbar\mu_1^2},$$

$$g_2^2=\frac{2\pi\omega_2 d_2^2 NG_2}{\hbar\mu_2^2}.$$

After substituting the expressions for the population differences into Eq. (12), we obtain

$$|e|\simeq\frac{|e_1||e_2|}{\gamma_{32}}\left(\frac{\omega}{\omega_1}\frac{d^2}{d_1^2}\frac{\kappa_1}{G_1}\frac{G}{\kappa}+\frac{\omega}{\omega_2}\frac{d^2}{d_2^2}\frac{\kappa_2}{G_2}\frac{G}{\kappa}\right), \tag{15}$$

or, in terms of field intensities,

$$|\mathcal{E}|^2\simeq|\mathcal{E}_1|^2\frac{|\mathcal{E}_2|^2}{|\mathcal{E}_2|_s^2}\left(\frac{d}{d_1}\frac{\omega}{\omega_1}\frac{\kappa_1}{G_1}\frac{G}{\kappa}\right)^2+|\mathcal{E}_2|^2\frac{|\mathcal{E}_1|^2}{|\mathcal{E}_1|_s^2}\left(\frac{d}{d_2}\frac{\omega}{\omega_2}\frac{\kappa_2}{G_2}\frac{G}{\kappa}\right)^2. \tag{16}$$

Here we introduced the quantity $|\mathcal{E}_{1,2}|_s^2$ defined as

$$|\mathcal{E}_{1,2}|_s^2 \equiv \hbar^2 \gamma_{32}^2 / d_{1,2}^2 . \tag{17}$$

Equation (17) represents the saturation intensity if we assume that all γ_{ik} in Eqs. (6) are equal and are of the same order that the inverse lifetime T_1^{-1} of carriers participated in generation. It seems to be approximately correct in QWs where the injection of carriers to the spectral region involved in the generation of a given mode is defined by the same scattering process as the relaxation of polarization. For QDs the relaxation mechanisms are less clear [14,23].

At a given wavelength the crucial parameter in Eq. (15), which governs the efficiency of down conversion, is $\eta = (\kappa_{1,2}/G_{1,2})(G/\kappa)$. The main source of the IR losses is free-carrier absorption. For the optical fields the ratio $\kappa_{1,2}/G_{1,2}$ is equal to the material gain at the optical transition, which is of order 10^3 cm^{-1} in QWs and 10^4 cm^{-1} in QDs. Therefore, even for very high IR material losses of order $10^3 - 10^4$ cm^{-1}, the η parameter can still be close to unity. As we already mentioned, IR losses can be dominated by absorption in doped cladding layers. Our detailed calculations for the GaAs-based structure with a separate confinement of IR ($\lambda = 8$ μm) and optical modes ($\lambda = 0.73$ and 0.8 μm) yield the value of η around $0.5-0.8$. Details will be published elsewhere.

The value of η decreases with increasing wavelength due to growing κ and decreasing G. Let us take as an example $2\kappa \simeq 150$ cm^{-1}, as measured in quantum cascade lasers at 17 μm wavelength. If $2\kappa_1/G_1 \simeq 1500$ cm^{-1}, then we have $\eta \sim 0.1$ for $G \sim 0.01$.

B. Inhomogeneous broadening

We will assume here that the inhomogeneous widths u_{ik} of all transitions are much larger than all homogeneous bandwidths γ_{ik} and Rabi frequencies $|e_{1,2}|$ of optical laser fields that are at exact resonance with the centers of inhomogeneously broadened lines: $\omega_1 = \omega_{21}$ and $\omega_2 = \omega_{31}$. We consider two different situations in which explicit formulas can be obtained: when the optical field intensities are (i) much smaller and (ii) much greater than the saturation values.

(i) In this case the populations have the spectral distributions as supported by pumping in the absence of generated fields (no spectral hole burning). When $u_{ik} \gg \gamma_{ik}$, the precise shape of the inhomogeneous line is not important and simple expression for the IR field can be obtained,

$$|e| \simeq \frac{2|e_1||e_2|}{(\gamma_{32}+\gamma_{21})} \frac{u_{21}}{u_{32}} \frac{\omega}{\omega_1} \frac{d^2}{d_1^2} \frac{\kappa_1}{G_1} \frac{G}{\kappa}, \tag{18}$$

or, in terms of intensities,

$$|\mathcal{E}|^2 \simeq |\mathcal{E}_1|^2 \frac{|\mathcal{E}_2|^2}{|\mathcal{E}_2|_s^2} \left(\frac{2\gamma_{32}}{(\gamma_{32}+\gamma_{21})} \frac{d}{d_1} \frac{\omega}{\omega_1} \frac{u_{21}}{u_{32}} \frac{\kappa_1}{G_1} \frac{G}{\kappa} \right)^2 . \tag{19}$$

Here $|\mathcal{E}_2|_s^2 = \hbar^2 \gamma_{32}^2 / d_2^2$. Equation (18) is similar to Eq. (15) except for the ratios of inhomogeneous linewidths that are expected to be of the order of unity. As we see, the ratio of the IR to optical intensity does not change much as compared with homogeneously broadened transitions, but, of course, the threshold conditions do change, so the value of the injection current is now much larger.

(ii) In this case the population distributions have narrow spectral holes burned at the spectral positions of optical field modes. This can be relevant for QD lasers or powerful pulsed multiple QW lasers. To simplify calculations, let us assume that the absolute values of the Rabi frequencies of two optical fields are equal, $|e_1| = |e_2|$, all γ_{ik} and r_i are equal to the same value γ, and also $u_{21} = u_{31} = u$.

Even with all these simplifications, the general solution for population differences is very cumbersome:

$$n_{12} + n_{13} = [(\overline{\rho}_{12} + \overline{\rho}_{13})A + 12\gamma |e_1|^4 \delta^2 |\Gamma|^2 \times (\overline{\rho}_{12} - \overline{\rho}_{13})] |\tilde{\Gamma}|^2 |\Gamma|^6 / D, \tag{20}$$

$$n_{12} - n_{13} = [(\overline{\rho}_{12} - \overline{\rho}_{13})B + 4\gamma |e_1|^4 \delta^2 |\Gamma|^2 \times (\overline{\rho}_{12} + \overline{\rho}_{13})] |\tilde{\Gamma}|^2 |\Gamma|^6 / D, \tag{21}$$

where

$$A = |\tilde{\Gamma}|^2 |\Gamma|^6 + 2|e_1|^2 |\tilde{\Gamma}|^2 |\Gamma|^4 + 4|e_1|^4 \delta^2 |\Gamma|^2 + 8|e_1|^6 \delta^2,$$

$$B = |\tilde{\Gamma}|^2 |\Gamma|^6 + 6|e_1|^2 |\tilde{\Gamma}|^2 |\Gamma|^4 + 12\gamma^2 |e_1|^4 (|\Gamma|^2 + 2|e_1|^2),$$

$$D = AB - 3(2|e_1|^2 \delta |\Gamma|)^4,$$

$$|\Gamma|^2 = \gamma^2 + \delta^2, \quad |\tilde{\Gamma}|^2 = \gamma^2 (1 + 2|e_1|^2 / |\Gamma|^2)^2 + \delta^2.$$

The expressions (20) and (21) have to be substituted into the right-hand sides of Eqs. (3), (4), and (12). After expanding the integrands in powers of a small parameter $\gamma/|e_1| \ll 1$ and retaining only the leading nonvanishing terms, we are left with a large number of integrals containing the ratios of different polynomials of δ. The functional dependence on all parameters of the problem can be extracted from integrals by the substitution of variables. Then the integrals are evaluated numerically giving just numerical factors in front of different terms. Many integrals cancel each other, and only the terms originated from the poles having the values $\delta \sim i|e_1|$ survive ($i^2 = -1$). This is to be expected since the widths of the spectral holes in the line profiles should be of order $|e_1|$. Summing all the remaining terms and rounding the numerical coefficients up to one digit, we arrive at a surprisingly simple result,

$$|e| \simeq \frac{|e_1||e_2|u}{\gamma u_{32}} \left| 0.9 \frac{g^2}{g_1^2} \frac{\kappa_1}{\kappa} - 0.1 \frac{g^2}{g_2^2} \frac{\kappa_2}{\kappa} \right| \tag{22}$$

or

$$|e| \simeq \frac{|e_1||e_2|u}{\gamma u_{32}} \left| 0.9 \frac{\omega}{\omega_1} \frac{d^2}{d_1^2} \frac{\kappa_1}{G_1} \frac{G}{\kappa} - 0.1 \frac{\omega}{\omega_2} \frac{d^2}{d_2^2} \frac{\kappa_2}{G_2} \frac{G}{\kappa} \right| . \tag{23}$$

In principle, the two terms in Eq. (22) can cancel each other if, e.g., the losses at frequency ω_2 are much larger than that at ω_1. (Of course, this would require taking into account other terms in the expansion over $\gamma/|e_1|$.) However, this can happen only if the pumping provides population inversion at the transition $3\rightarrow 2$. This is clear from the expression for the population difference at the center of the transition $3\rightarrow 2$, supported by pumping in the absence of generation,

$$\overline{\rho}_{23}(\delta=0)\simeq\frac{|e_1|u}{\gamma^2}\left(1.5\frac{\kappa_1}{g_1^2}-1.1\frac{\kappa_2}{g_2^2}\right). \tag{24}$$

For the transition between the ground subband and a higher subband, the population inversion is unlikely to be achieved at reasonable pumping rates.

The requirement $e<\gamma$ employed in the derivation of Eq. (9) necessarily means that $|e|\ll|e_1|$ in the asymptotics (22), since the latter was obtained in the limit $|e_1|\gg\gamma$.

Expressions (16),(19),(23) predict the rapid growth of the IR intensity, proportional to the product of optical field intensities. Of course, this tendency holds only until the IR intensity reaches the saturation value. Above this value, the IR field begins to deplete the electron populations, and its growth becomes nonlinearly saturated. In the optimal case, the maximum internal efficiency of the down conversion can reach the limiting quantum value corresponding to one IR photon per one optical photon.

For the mid-IR range $5-10$ μm the maximum IR power is of order 10 mW if we take the value of 100 cm^{-1} for IR losses. Here we assumed the laser with parameter $\eta\sim 0.1$; see the discussion after Eq. (15). Beyond the reststrahlen region of strong phonon dispersion ($\lambda\gtrsim 50$ μm for $Al_xGa_{1-x}As/GaAs$ structure) the expected IR power is $\lesssim 1$ mW due to rapidly growing losses. We note, however, that progress in fabricating low-loss IR waveguides for semiconductor lasers is impressive. For example, in [24] waveguide losses as low as 14 cm^{-1} at 9.5-μm wavelength were reported.

V. CONCLUSIONS

Our calculations demonstrate the generation of coherent IR emission at intersubband transitions due to nonlinear wave mixing in standard multiple-QW or -QD laser diodes. The prerequisite for this is simultaneous lasing at two optical wavelengths which provide the necessary drive fields. This mechanism does not require population inversion at the IR transition, and its threshold current is determined by the minimum injection current necessary for the interband lasing from higher (excited) carrier states of dimensional quantization.

It is important to note that the proposed parametric scheme seems to be viable in the far-IR region ($\lambda\sim 10-100$ μm) using transitions between hole subbands in the valence band. Indeed, in conventional lasers the increase of IR losses with wavelength is a significant problem for generation since it becomes difficult to reach the lasing threshold. In our case, due to the parametric nature of IR generation, the increase in losses will only lead to a decrease in output intensity; not a complete loss of IR generation as is the case in the usual below-threshold laser behavior. For a practical device, the goal is to maximize the factor $(\kappa_{1,2}/G_{1,2})(G/\kappa)$. Also, in the far-IR spectral range it is relatively easy to manipulate the refractive index of the IR mode and provide phase matching by only a modest doping of waveguide layers.

ACKNOWLEDGMENTS

We gratefully acknowledge encouraging and helpful discussions with D. Depatie, R. Haden, Yu. Rostovtsev, and H. Taylor and thank the Office of Naval Research, the National Science Foundation, the Robert A. Welch Foundation, and the Texas Advanced Technology Program for their support.

[1] R.F. Kazarinov and R.A. Suris, Fiz. Tekh. Poluprovodn. **5**, 797 (1971) [Sov. Phys. Semicond. **5**, 707 (1971)].
[2] J. Faist, F. Capasso, D. L. Sivco, C. Sirtori, A. L. Hutchinson, and A. Y. Cho, Science **264**, 553 (1994).
[3] J. Singh, IEEE Photonics Technol. Lett. **8**, 488 (1996).
[4] *Semiconductor Lasers*, edited by E. Kapon (Academic Press, San Diego, 1999).
[5] *Intersubband Transitions in Quantum Wells: Physics and Devices*, edited by S. S. Li and Y.-K. Su (Kluwer, Boston, 1998).
[6] F. Capasso, C. Gmachl, A. Tredicucci, A. L. Hutchinson, D. L. Sivco, and A. Y. Cho, Opt. Photonics News **10**, 33 (1999).
[7] Liu *et al.*, in *Nonlinear Optics: Materials, Fundamentals and Applications*, OSA Technical Digest (Optical Society of America, Washington, D.C., 2000), p. 56.
[8] S.E. Harris, Phys. Rev. Lett. **62**, 1033 (1989); O. Kocharovskaya and Ya.I. Khanin, Pis'ma Zh. Éksp. Teor. Fiz. **48**, 536 (1988) [JETP Lett. **48**, 580 (1988)]; M.O. Scully, S.-Y. Zhu, and A. Gavrielides, Phys. Rev. Lett. **62**, 2813 (1989); for a review, see, e.g., O. Kocharovskaya, Phys. Rep. **219**, 175 (1992); M. O. Scully and M. S. Zubairy, *Quantum Optics* (Cambridge University Press, Cambridge, 1997).
[9] A. Imamoglu, R.J. Ram, Opt. Lett. **19**, 1744 (1994); H. Schmidt, D. E. Nikonov, K. L. Campman, K. D. Maranowski, A. C. Gossard, and A. Imamoglu, Laser Phys. **9**, 797 (1999).
[10] A. Zibrov *et al.* (unpublished).
[11] J. Vanier, A. Godone, and F. Levi, Phys. Rev. A **58**, 2345 (1998).
[12] E.A. Korsunsky and D.V. Kosachov, J. Opt. Soc. Am. B **17**, 1405 (2000).
[13] F. Bassani and G. Pastori Parravicini, *Electronic States and Optical Transitions in Solids* (Pergamon Press, Oxford, 1975).
[14] D. Bimberg, M. Grundmann, and N. N. Ledentsov, *Quantum Dot Heterostructures* (Wiley & Sons, New York, 1998).
[15] Y. Tokuda, N. Tsukada, K. Fujiwara, and T. Nakayama, Appl.

Phys. Lett. **49**, 1629 (1986).
[16] T.R. Chen, Y. Zhuang, Y. J. Xu, B. Zhao, A. Yariv, J. Ungar, and Se Oh, Appl. Phys. Lett. **60**, 2954 (1992).
[17] W. W. Chow and S. W. Koch, *Semiconductor-Laser Fundamentals* (Springer, Berlin, 1999).
[18] O. Kocharovskaya, P. Mandel, and Y.V. Radeonychev, Phys. Rev. A **45**, 1997 (1992).
[19] A. Belyanin, C. Bentley, F. Capasso, O. Kocharovskaya, and M. O. Scully (unpublished).
[20] M. Asada, IEEE J. Quantum Electron. **25**, 2019 (1989).
[21] M. Hartig, J. D. Ganiere, P. E. Selbmann, B. Devaud, and L. Rota, Phys. Rev. B **60**, 1500 (1999).
[22] B. Jensen, in *Handbook of Optical Constants of Solids*, edited by E. D. Palik (Academic, Orlando, FL, 1985).
[23] A.V. Uskov, K. Nishi, and R. Lang, Appl. Phys. Lett. **74**, 3081 (1999).
[24] C. Sirtori, P. Kruck, S. Barbieri, H. Page, J. Nagle, M. Beck, J. Faist, and U. Oesterle, Appl. Phys. Lett. **75**, 3911 (1999).